

Controllable Supramolecular Architectures for Modulating Optical Properties on the Molecular Aggregation Level

Runsheng Jiang,^[a,b] Zheng Xue,^[c] Yongjun Li,^{*,[a]} Zhihong Qin,^[a,b] Yuliang Li,^{*,[a]} and Daoben Zhu^[a]

Keywords: Conjugation / Nanostructures / Nanoparticles / Charge transfer / Solid-state structures

Driven by the association of chemical weak forces and solvent effects, zero- to two-dimensional nanostructures of thiophene-substituted perylene bisimide such as spheres and blocky structures were obtained. Light-controlled intramo-

lecular charge transfer from the trithiophene unit to the perylene bisimide in the solid state can induce a hypochromatic shift and enhanced fluorescent emission.

Introduction

In recent years, perylenetetracarboxylic acid diimides (PDI) have been extensively studied as building blocks for functional supramolecular architectures through hydrogen bonding, metal ion coordination, and π - π stacking interactions.^[1] Due to their outstanding optical and electronic properties, especially upon formation of aggregated nanostructures,^[2] PDI has been widely used for electronic materials,^[3] organic solar cells,^[4] photoluminescence,^[5] sensors,^[6] organic light-emitting diodes,^[7] field-effect transistors,^[8] dye lasers,^[9] liquid crystalline materials,^[10] and molecular switches.^[11] In particular, there is growing interest in the design of PDI systems that can self-assemble into uniform aggregates with specific shape and novel functionalities. Indeed, an effective way to shape supramolecular architectures is through molecular self-assembly technology based on intramolecular, intermolecular, and molecule-substrate interactions.

With the aim of improving the performance of PDI as a functional material in devices, a great deal of interest has been stimulated in the past decade in modifying PDI molecules to tune the photophysical and redox properties of the systems and to enhance their ability to self assemble.^[12] Such molecular modification can be achieved by expanding

the π -conjugation either along the long molecular axis from perylene to hexarylene diimides, which induces a significant bathochromic shift, or along the short axis at the bay positions of the aromatic core, resulting in a hypsochromic shift.^[13] Understanding the structure-property relationships that relate specifically to aggregate nanostructures and materials is critical for the development of new architectures for benign, high-performance conjugated molecules.^[14,15]

To derive different properties from individual molecules, tuning the self-assembly process is an effective method.^[16] The optical properties of the conjugated molecules can also be influenced by different conformations and spatial arrangements, such as observed in conformation-dependent fluorescent enhancement induced by laser irradiation.^[17]

Here, we report a PDI derivative bridged by trithiophenes that shows a hypochromatic shift and fluorescent enhancement upon UV light irradiation on the aggregated level. The changes are realized by tuning the intramolecular

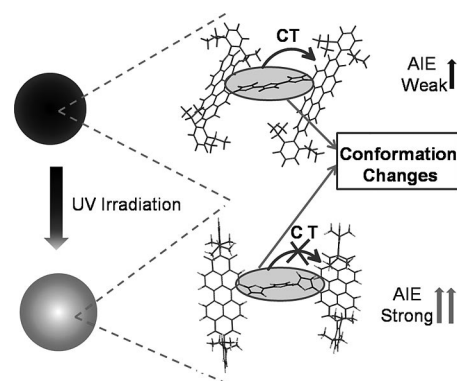


Figure 1. Schematic interpretation of the hypochromatic shift and enhanced emission observed in thiophene-bridged perylene bisimide supramolecular architectures.

[a] Beijing National Laboratory for Molecular Sciences (BNLMS), CAS Key Laboratory of Organic Solids, Institute of Chemistry, Chinese Academy of Sciences, Beijing 100190, P. R. China
E-mail: ylli@iccas.ac.cn
lij@iccas.ac.cn
http://www.iccas.ac.cn

[b] Graduate University of Chinese Academy of Sciences, Beijing 100049, P. R. China

[c] State Key Laboratory for Supramolecular Structures and Materials, College of Chemistry, Jilin University, Changchun 130012, P. R. China

Supporting information for this article is available on the WWW under <http://dx.doi.org/10.1002/ejoc.201402460>.

FULL PAPER

charge transfer (ICT) from the trithiophene unit to the perylene bisimide through light-induced conformation changes of the trithiophene moieties (Figure 1).

Results and Discussion

As shown in Scheme 1, the Suzuki reaction of 1-bromoperylene-tetracarboxylic acid diimide and 2,2'-trithiophene-5,5'-diboronic acid bis(pinacol) ester smoothly afforded thiophene-substituted compound **2** in 60% yield upon heating to reflux overnight. Compound **2** was characterized by ^1H NMR, ^{13}C NMR and high-resolution MALDI-TOF MS analyses.

The measured redox potentials for thiophene-substituted perylene are shown in Table S1 (see the Supporting Information). Compound **2** exhibits two reversible one-electron oxidation peaks at 1.19 and 1.43 V. The first oxidation potential of **2** is 0.53 V lower than that of the parent PDI, indicating that attachment of the trithiophene group to the perylenetetracarboxylic acid diimide makes the molecule easier to oxidize. Compound **2** shows two reversible reduction potentials at -0.56 and -0.80 V (vs. SCE), and no significant shift was observed compared with the parent PDI. From the HOMO (-5.59 eV) and LUMO (-3.84 eV) energy levels and the corresponding energy gap (1.75 eV), the π -electron-rich thiophene unit effectively extends the π -conjugation system of **2**, raising the HOMO level and leaving the LUMO level unchanged, resulting in a smaller energy gap compared with that of the parent PDI (2.15 eV).

The absorption and fluorescence spectra of **2** in dichloromethane (CH_2Cl_2) at room temperature are shown in Figure 2, which reveals the perylene core π - π^* transition absorption bands around 510 nm ($\epsilon_{\text{max}} = 26400 \text{ M}^{-1} \text{ cm}^{-1}$) and thiophene unit absorption at 378 nm, as well as a shoulder charge-transfer band around 550–700 nm (the latter band does not change with concentration, see Figure S3 in the Supporting Information). Compared with the parent PDI ($\lambda_{\text{max}} = 528$ nm), the maximum absorption value of **2** showed a blueshift of 18 nm. Excitation at the absorption band of the perylene bisimide unit led to emission at 572 nm, with a fluorescence quantum yield of 0.37. The emission spectra of **2** excited at the thiophene unit (360 nm) are shown in Figure 3, which reveals two clear fluorescent emissions (430 and 540 nm). The emission peak at 430 nm

arises from the thiophene units, and the peak at 540 nm originates from the PDI units. Particularly in the concentration range of 0 to 1×10^{-6} M, the emission of PDI unit was quenched due to ICT from the trithiophene unit to the perylene bisimide. When the concentration was higher than 1×10^{-6} M, although the emission of thiophene units (409 nm) started to decrease due to stacking effects, the emission of the PDI units (540 nm) appeared, because the aggregation-induced emission effect (AIE) of the perylene bisimide unit compensates for the ICT from the trithiophene unit to the perylene bisimide (Figure 3).

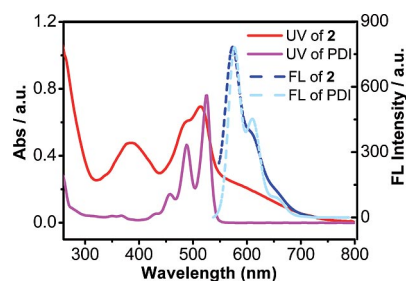


Figure 2. Absorption and emission (excited at 480 nm) spectra of **2** and PDI in CH_2Cl_2 (1×10^{-6} M) at room temperature.

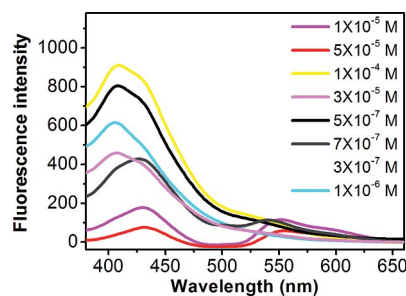
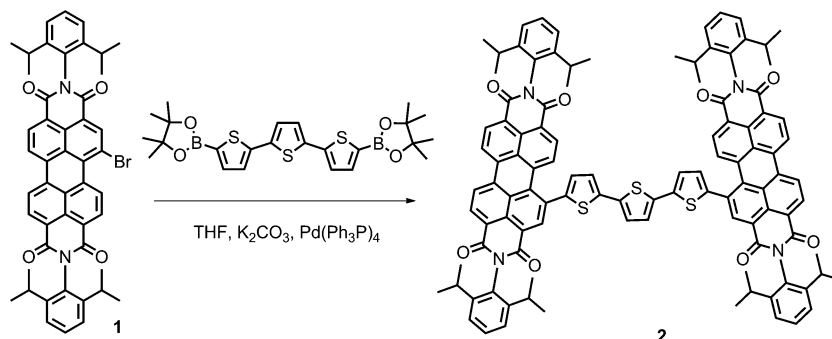


Figure 3. Emission spectra (excited at 360 nm) of **2** in CH_2Cl_2 at different concentrations.

To study the aggregation ability of **2** (which dissolved in CH_2Cl_2 at a concentration of 1.0×10^{-4} M), self-assembly was carried out in a range of solvents such as hexane or acetone after optimization. Typical SEM and TEM images of the nano- and micro-aggregate structures of **2** with different morphologies are shown in Figure 4. Self-assembly in CH_2Cl_2 /hexane leads to regular nanospheres (Figure 4a). The SEM images of **2** (Figure 4c) assembled in CH_2Cl_2 /



Scheme 1. Synthesis of the thiophene-substituted perylene diimide.

acetone (1:1, v/v) show a highly regular blocky structure with approximately 3 μm length and 400 nm thickness (Figure S4); its TEM images are shown in Figure 4d.

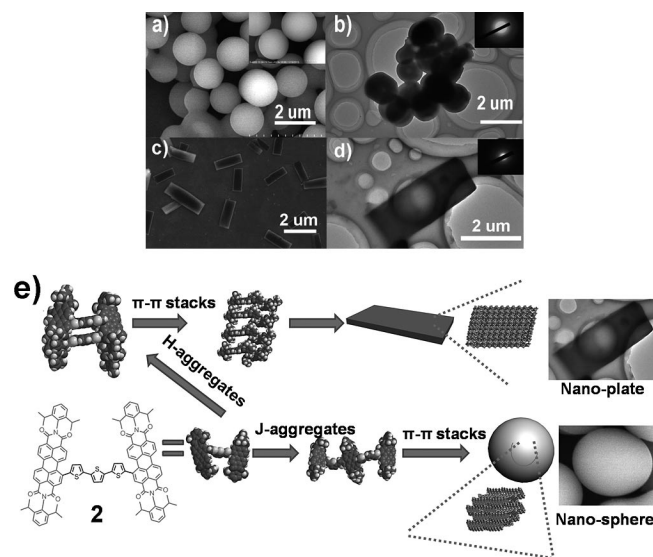


Figure 4. (a) SEM and (b) TEM images of **2** assembled in CH_2Cl_2 /hexanes (1:1) at room temperature; (c) SEM and (d) TEM images of **2** assembled in CH_2Cl_2 /acetone (1:1, v/v) at room temperature. (e) Proposed mechanism for the supramolecular organization of **2**.

As shown in Figure 5, the absorption and emission spectra of the self-assembled nanostructures from CH_2Cl_2 /hexane (v/v, 1:1) were redshifted compared with those from structures obtained from CH_2Cl_2 , which indicated that the nanospheres formed in this condition were J-type aggregated (Figure 4e). In the mixed CH_2Cl_2 /acetone solvents, blueshifted absorption and emission spectra were observed,

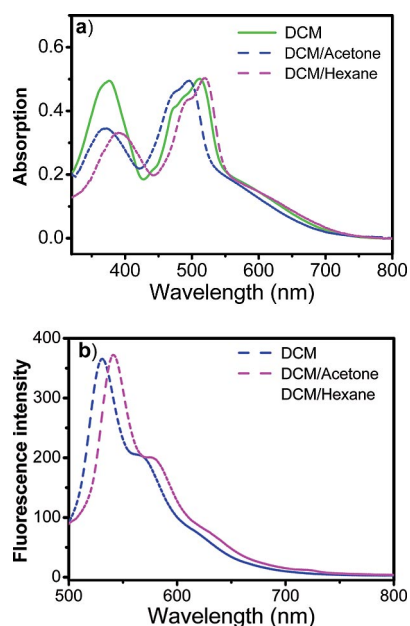


Figure 5. Normalized (a) absorption and (b) emission (excited at 480 nm) spectra of aggregations of compound **2** from CH_2Cl_2 and mixed solvents CH_2Cl_2 /acetone and CH_2Cl_2 /hexane.

which indicated that H-type aggregation occurred in the blocky structures (Figure 4e).

The optical properties of these nanostructures prepared from **2** were further studied with a laser scanning confocal microscope (LSCM). Nanostructures of **2** showed weak solid emission around 750 nm, which is related to the charge-transfer band. It was found that the emission of these aggregates showed a blueshift of about 170 nm upon 405 nm wavelength irradiation, accompanied by enhanced fluorescence intensity upon extended UV irradiation (Figure 6d–e). The time-dependent fluorescent spectra of the nanospheres of **2** with 405 nm UV irradiation are shown in Figure 6f. This process is very fast: 2.5 min irradiation led to complete emission shifts from 750 to 580 nm. In addition, self-assembled samples with other morphologies, such as nanoslices, also exhibit the same phenomena of blueshifted and enhanced fluorescence upon extended UV irradiation (Figure 6b). Spin-coated films without self-assembly did not show blueshifted emission upon UV light irradiation (Figure S5).

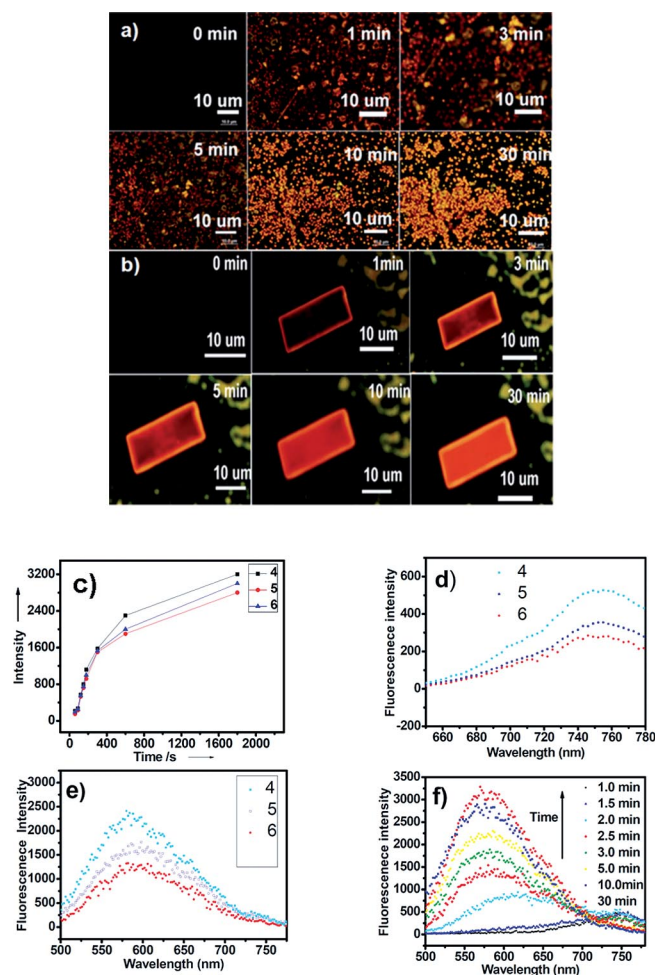


Figure 6. (a and b) LSCM of **2** under 405 nm UV irradiation. (c) Time-dependent intensity plot of the fluorescence emission of **2** (d) before and (e) after UV irradiation for 5 min. (f) Time-dependent emission spectra of self-assembled **2** under UV irradiation (the numbers 4, 5 and 6 represent the different chosen areas on the cover glass).

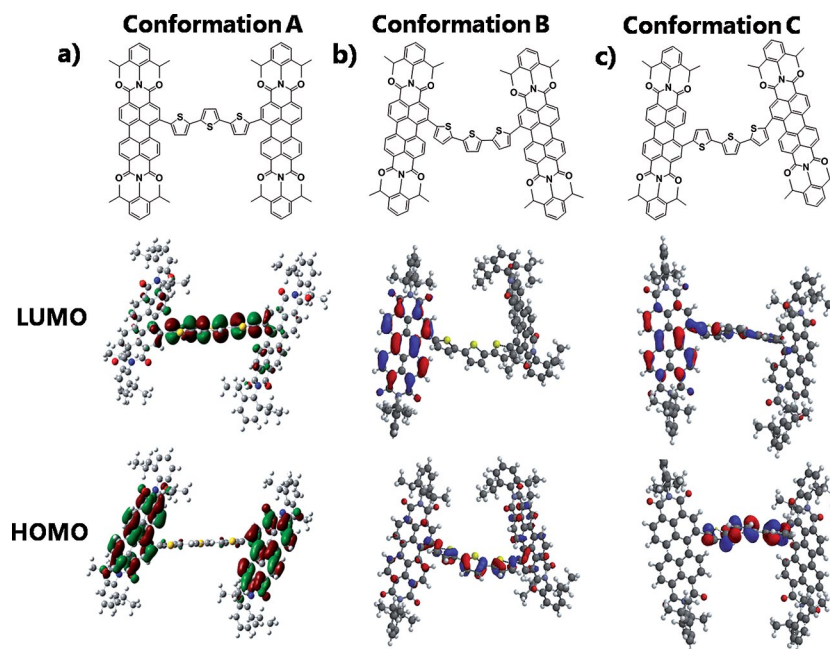


Figure 7. Calculated spatial distributions of HOMO and LUMO for **2** at the B3LYP/6-31G(d,p) level on conformations A, B and C, calculated with Spartan programs.

The conformation of compound **2** varies significantly when going from an isolated molecule (in which the single bond connecting the perylene bisimide unit and the thiophene group can rotate freely) to the solid state (in which the rotation is locked by packing effects), thus generating different chemical environments owing to specific intermolecular interactions. In the solid state, conformation constraints limit the rotation of the perylene bisimide groups due to packing effects. However, the thiophene units can still flip within the cavity provided by the bulky perylene bisimide terminals. The most stable conformation for **2** is when the three thiophene rings are located on a plane with crosswise packing, which is identical to the same part of the most stable thermodynamic conformation A (with the minimization energy of -6184.1864 a.u.) of **2** obtained by the calculations (Figure 7a).^[18] The densities in the HOMO orbitals are concentrated on the thiophene ring moiety, whereas the densities in the LUMO orbitals delocalize on both PDI units, which means that intramolecular charge transfer takes place from the thiophene to the perylene bisimide, as evidenced by the shoulder absorption of **2** in the 550–700 nm region. With sufficient energy (excitation at 405 nm, the frequency at which thiophene units absorb), the thiophene rings in the nonfused trithiophene unit can rotate to the less stable conformations B and C (with minimized energy of -6311.7275 a.u. and -6209.0661 a.u., respectively), in which the electron-donating ability of the trithiophene unit decreases and the HOMO and LUMO orbital distributions also change (Figure 7b–7c). In contrast to the situation with conformation A, the LUMO orbitals of conformations B and C are mainly concentrated on one of the PDI units, which indicates that conformation A has a stronger ICT tendency. For the nanosphere film of **2**, the

absorbance of the thiophenes at 380 nm decreased upon UV irradiation, which supports the conclusion that a conformational change occurs around the oligothiophene moiety. The thiophene rings in the nonfused trithiophene unit rotate to the less stable conformations B and C, which decreases the extent of conjugation of the trithiophene unit and leads to less ICT (a small decrease was observed for the ICT absorption band around 550–700 nm; Figure S6).

Solid-state effects can potentially slow down nonradiative decay pathways that involve conformational degrees of freedom, which is a phenomenon known as AIE. The weak emission of **2** in solution is attributed to ICT from the trithiophene unit to the perylene bisimide and to intramolecular rotation of the perylene bisimide rings around the thiophene rings. Strong emission in the solid state would be expected to result from restriction of intramolecular rotation. Therefore, it is expected that, with obstruction of the charge transfer from the thiophene units to the perylene bisimide, the characteristic AIE phenomena of bulky perylene bisimide terminals would be enhanced, that is, the emission at 750 nm would be expected to disappear and the emission at 580 nm should increase.

Conclusions

A thiophene-substituted perylene bisimide has been synthesized and used to demonstrate a relatively simple associated approach to the construction of nano- and microstructures with zero and two dimensions. The thiophene-substituted perylene bisimide showed conformation-dependent hypochromatic shift and fluorescent enhancement behavior in the solid state, which is induced by tuning the

intramolecular charge transfer from the trithiophene unit to the perylene bisimide through light-induced conformation changes of the trithiophenes. The mechanism differs from the fluorescent bleaching of normal solid-state fluorescent materials, and suggests potentially important applications in optical devices. This work demonstrates the importance of controlling molecular conformation in molecular aggregation systems to modulate optical properties.

Experimental Section

General Methods: *N,N'*-Bis(2,6-diisopropylphenyl)-1-bromoperylene-3,4,9,10-tetracarboxylic acid diimide and 2,2'-([2,2':5',2''-terthiophene]-4,5''-diyl)bis(4,4,5,5-tetramethyl-1,3,2-dioxaborolane) were synthesized according to the literature.^[20] ¹H NMR (400 MHz) spectra were recorded in deuterated solvents with a Bruker Avance 400 NMR spectrometer. ¹³C NMR (100 MHz) spectra were recorded with a Bruker Avance 400 NMR spectrometer. Mass spectra (MALDI-TOF-MS) were determined with a Bruker Biflex III mass spectrometer. Electronic absorption spectra were measured with a JASCO V-579 spectrophotometer in a quartz cell. Fluorescence excitation and emission spectra were recorded with a Hitachi F-4500 spectrometer at room temperature. Fluorescence quantum yields were determined by using the optical dilute method with *N,N'*-bis(2,6-diisopropylphenyl)perylene-3,4,9,10-tetracarboxylic acid diimide (PDI) in CH₂Cl₂ as reference ($\Phi_{fl} = 1.0$). Cyclic voltammograms (CVs) were recorded with a CHI660D electrochemical workstation at a scan rate of 100 mV s⁻¹, with glassy carbon electrode as the working electrode, Pt wire as the counter electrode, and an SCE as the reference electrode. 0.1 M tetrabutylammonium hexafluorophosphate (Bu₄NPF₆) in dichloromethane (CH₂Cl₂; HPLC grade) was employed as the supporting electrolyte.

Calculations for Cyclic Voltammograms: According to de Leeuw et al.,^[19] when using SCE as the reference electrode, the energy levels (in eV) can be obtained as following: $E_{LUMO} = -e(E_{red} + 4.4)$ (eV) and $E_{HOMO} = -e(E_{ox} + 4.4)$ (eV), where E_{LUMO} and E_{HOMO} correspond to the LUMO energy level and the HOMO energy level, respectively; E_{ox} and E_{red} are the onset potentials determined by the intersection of the two tangents drawn at the rising oxidation (or reduction) current and background current in the cyclic voltammograms. The energy gap can be obtained by $E_g = e[E_{ox} - E_{red}]$ (eV).

Compound 2: A Schlenk flask was charged with **1** (100 mg, 0.125 mmol), 2,2'-([2,2':5',2''-terthiophene]-4,5''-diyl)bis(4,4,5,5-tetramethyl-1,3,2-dioxaborolane) (31 mg, 0.063 mmol), THF (10 mL), and a 2 M solution of potassium carbonate (2 mL) in water under argon. After 10 min, [Pd(PPh₃)₄] (10 mg, 0.013 mmol) was added, and the mixture was stirred at 75 °C overnight. After cooling to room temperature, the mixture was diluted with dichloromethane and washed with water and saturated NaCl (aq.). Upon drying with anhydrous Na₂SO₄, the organic layer was concentrated in vacuo, and the crude product was purified by column chromatography on silica gel (CH₂Cl₂/petroleum ether, 1:2 to 4:1, v/v) to afford **2** (62 mg, 60%) as a deep-red solid. ¹H NMR (CD₂Cl₂, 400 MHz): δ = 8.78 (m, 10 H), 8.56–8.54 (m, J = 7.3 Hz, 2 H), 8.40–8.38 (d, J = 7.7 Hz, 2 H), 7.58 (m, 4 H), 7.42 (m, 12 H), 7.19 (s, 1 H), 2.73 (m, 8 H), 1.13–1.11 (m, 24 H, isopropyl-H) ppm. ¹³C NMR (CD₂Cl₂, 100 MHz): δ = 164.1, 164.0, 163.8, 146.5, 142.9, 137.2, 135.8, 135.6, 135.2, 133.9, 132.0, 131.5, 131.4, 131.2, 130.3, 130.1, 130.0, 129.9, 129.8, 128.7, 128.4, 127.3, 125.6, 125.5, 125.3, 124.9, 124.6, 124.5, 124.5, 124.4, 123.8, 123.7, 123.5,

123.1, 122.7, 30.1, 29.5, 24.2 ppm. IR (KBr): $\tilde{\nu}$ = 2961, 2925, 2868, 1706, 1667, 1590, 1457, 1401, 1339, 1248, 1199, 970, 813 cm⁻¹. HRMS (MALDI-TOF): calcd. for C₁₀₈H₈₈N₄O₈NaS₃ [M + Na⁺] 1687.56565; found 1687.56563.

Supporting Information (see footnote on the first page of this article): UV/Vis and fluorescence spectra, ¹H NMR, ¹³C NMR and HR mass (MALDI TOF) spectra for final product **2**.

Acknowledgments

This work was supported by the National Nature Science Foundation of China (21031006, 91227113, and 21322301), the NSFC-DFG joint fund (TRR 61), the National Basic Research 973 Program of China (2011CB932302 and 2012CB932900), and the “Strategic Priority Research Program” of the Chinese Academy of Sciences (XDA01020304).

- a) T. van der Boom, R. T. Hayes, Y. Y. Zhao, P. J. Bushard, E. A. Weiss, M. R. Wasielewski, *J. Am. Chem. Soc.* **2002**, *124*, 9582–9590; b) H. Liu, J. L. Xu, Y. Li, Y. Li, *Acc. Chem. Res.* **2010**, *43*, 1496–1508; c) M. R. Wasielewski, *Acc. Chem. Res.* **2009**, *42*, 1910–1921.
- a) M. Supur, Y. Yamada, S. Fukuzumi, *J. Mater. Chem.* **2012**, *22*, 12547–12552; b) M. Supur, S. Fukuzumi, *J. Phys. Chem. C* **2012**, *116*, 23274–23282; c) M. Supur, S. Fukuzumi, *Phys. Chem. Chem. Phys.* **2013**, *15*, 2539–2546.
- a) B. A. Jones, M. J. Ahrens, M.-H. Yoon, A. Facchetti, T. J. Marks, M. R. Wasielewski, *Angew. Chem. Int. Ed.* **2004**, *43*, 6363–6366; *Angew. Chem.* **2004**, *116*, 6523; b) C. D. Dimitrakopoulos, P. R. Malenfant, *Adv. Mater.* **2002**, *14*, 99–117; c) A. L. Briseno, S. C. B. Mannsfeld, C. Reese, J. M. Hancock, Y. Xiong, S. A. Jenekhe, Z. Bao, Y. Xia, *Nano Lett.* **2007**, *7*, 2847–2853.
- a) P. Peumans, S. Uchida, S. R. Forrest, *Nature* **2003**, *425*, 158–162; b) M. L. Schmidt, A. Fechtenkötter, K. Müllen, E. Moons, R. H. Friend, J. D. MacKenzie, *Science* **2001**, *293*, 1119–1122.
- H. Langhals, J. Karolin, L. A. Johansson, *J. Chem. Soc. Faraday Trans.* **1998**, *94*, 2919–2922.
- N. I. Georgiev, A. R. Sakr, V. B. Bojinov, *Dyes Pigm.* **2011**, *91*, 332–339.
- a) C. Ego, D. Marsitzky, S. Becker, J. Y. Zhang, A. C. Grimsdale, K. Mullen, J. D. MacKenzie, C. Silva, R. H. Friend, *J. Am. Chem. Soc.* **2003**, *125*, 437–443; b) M. D. Damaceanu, C. P. Constantiu, M. Bruma, M. Pinteala, *Dyes Pigm.* **2013**, *99*, 228–239; c) L. C. Meng, Y. B. Hou, Z. D. Lou, F. Teng, X. Yao, X. J. Liu, A. W. Tang, J. B. Peng, *Synth. Met.* **2013**, *172*, 63–68.
- a) Z. Chen, Y. Zheng, H. Yan, A. Facchetti, *J. Am. Chem. Soc.* **2009**, *131*, 8–9; b) B. A. Jones, A. Facchetti, M. R. Wasielewski, T. J. Marks, *J. Am. Chem. Soc.* **2007**, *129*, 15259–15278.
- R. Gvishi, R. Reisfeld, Z. Burshtein, *Chem. Phys. Lett.* **1993**, *213*, 338–344.
- a) W. Pisula, M. Kastler, D. Wasserfallen, J. W. F. Robertson, F. Nolde, C. Kohl, K. Müllen, *Angew. Chem. Int. Ed.* **2006**, *45*, 819–823; *Angew. Chem.* **2006**, *118*, 834; b) A. Wicklein, A. Lang, M. Muth, M. Thelakkat, *J. Am. Chem. Soc.* **2009**, *131*, 14442–14453.
- Y. Li, H. Li, Y. Li, H. Liu, S. Wang, X. He, N. Wang, D. Zhu, *Org. Lett.* **2005**, *7*, 4835–4838.
- a) H. Liu, Y. Li, S. Xiao, H. Gan, T. Jiu, H. Li, L. Jiang, D. Zhu, D. Yu, B. Xiang, Y. Chen, *J. Am. Chem. Soc.* **2003**, *125*, 10794–10795; b) V. Palermo, S. Morelli, M. Palma, C. Simpson, F. Nolde, A. Herrmann, K. Mullen, P. Samori, *ChemPhysChem* **2006**, *7*, 847–853; c) L. Yang, H. Peng, K. Huang, J. T. Mague, H. B. Li, Y. Lu, *Adv. Funct. Mater.* **2008**, *18*, 1526–1535.

FULL PAPER

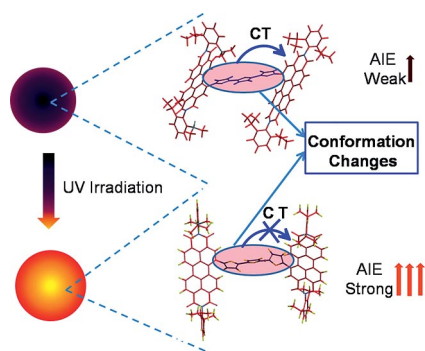
R. Jiang, Z. Xue, Y. Li, Z. Qin, Y. Li, D. Zhu

- [13] a) A. Sautter, C. Thalacker, F. Würthner, *Angew. Chem. Int. Ed.* **2001**, *40*, 4425–4428; *Angew. Chem.* **2001**, *113*, 4557; b) Y. Li, Z. Qing, Y. Yu, T. Liu, R. Jiang, Y. Li, *Chem. Asian J.* **2012**, *7*, 1934–1939; c) C. Zhan, A. D. Li, *Curr. Org. Chem.* **2011**, *15*, 1314–1339.
- [14] a) Y. Geerts, H. Quante, H. Platz, R. Mahrt, M. Hopmeier, A. Bohm, K. Mullen, *J. Mater. Chem.* **1998**, *8*, 2357–2369; b) F. O. Holtrup, R. J. Müller, H. Quante, S. De Feyter, F. C. De Schryver, K. Müllen, *Chem. Eur. J.* **1997**, *3*, 219–225.
- [15] a) Y. Li, L. Xu, T. Liu, Y. Yu, H. Liu, Y. Li, D. Zhu, *Org. Lett.* **2011**, *13*, 5692–5695; b) Y. Li, H. Zheng, Y. Li, S. Wang, Z. Wu, P. Liu, Z. Gao, H. Liu, D. Zhu, *J. Org. Chem.* **2007**, *72*, 2878–2885.
- [16] a) J. Lv, Y. Zhao, G. Li, Y. Li, H. Liu, Y. Li, D. Zhu, S. Wang, *Langmuir* **2009**, *25*, 11351–11357; b) L. Zhao, W. Yang, Y. Ma, J. Yao, Y. Li, H. Liu, *Chem. Commun.* **2003**, *19*, 2442–2443; c) Y. Liu, S. Xiao, H. Li, Y. Li, H. Liu, F. Lu, J. Zhuang, D. Zhu, *J. Phys. Chem. B* **2004**, *108*, 6256–6260.
- [17] Y. Yu, Q. Shi, Y. Li, T. Liu, L. Zhang, Z. Shuai, Y. Li, *Chem. Asian J.* **2012**, *7*, 2904–2911.
- [18] M. J. Frisch, G. W. Trucks, H. B. Schlegel, G. E. Scuseria, M. A. Robb, J. R. Cheeseman, J. A. Montgomery, J. T. Vreven, K. N. Kudin, J. C. Burant, J. M. Millam, S. S. Iyengar, J. Tomasi, V. Barone, B. Mennucci, M. Cossi, G. Scalmani, N. Rega, G. A. Petersson, H. Nakatsuji, M. Hada, M. Ehara, K. Toyota, R. Fukuda, J. Hasegawa, M. Ishida, T. Nakajima, Y. Honda, O. Kitao, H. Nakai, M. Klene, X. Li, J. E. Knox, H. P. Hratchian, J. B. Cross, V. Bakken, C. Adamo, J. Jaramillo, R. Gomperts, R. E. Stratmann, O. Yazyev, A. J. Austin, R. Cammi, C. Pomelli, J. W. Ochterski, P. Y. Ayala, K. Morokuma, G. A. Voth, P. Salvador, J. J. Dannenberg, V. G. Zakrzewski, S. Dapprich, A. D. Daniels, M. C. Strain, O. Farkas, D. K. Malick, A. D. Rabuck, K. Raghavachari, J. B. Foresman, J. V. Ortiz, Q. Cui, A. G. Baboul, S. Clifford, J. Cioslowski, B. B. Stefanov, G. Liu, A. Liashenko, P. Piskorz, I. Komaromi, R. L. Martin, D. J. Fox, T. Keith, M. A. Al-Laham, C. Y. Peng, A. Nanayakkara, M. Challacombe, P. M. W. Gill, B. Johnson, W. Chen, M. W. Wong, C. Gonzalez, J. A. Pople, *Gaussian 03*, Revision C.02, Gaussian, Inc., Wallingford, CT, **2004**.
- [19] D. M. de Leeuw, M. M. J. Simenon, A. R. Brown, R. E. F. Ein-erhand, *Synth. Met.* **1997**, *87*, 53–59.
- [20] Y. Geerts, H. Quante, H. Platz, R. Mahrt, M. Hopmeier, A. Bohm, K. Müllen, *J. Mater. Chem.* **1998**, *8*, 2357–2369.

Received: April 21, 2014

Published Online: ■

Light-controlled intramolecular charge transfer from the trithiophene unit to the perylene bisimide in the solid state can induce a hypochromatic shift and enhanced fluorescent emission.



R. Jiang, Z. Xue, Y. Li,* Z. Qin, Y. Li,*
D. Zhu 1–7

Controllable Supramolecular Architectures
for Modulating Optical Properties on the
Molecular Aggregation Level 

Keywords: Conjugation / Nanostructures /
Nanoparticles / Charge transfer / Solid-
state structures